JEE Journal of Ecological Engineering

Journal of Ecological Engineering, 2025, 26(5), 159–169
https://doi.org/10.12911/22998993/200062
ISSN 2299–8993, License CC-BY 4.0

Received: 2024.12.31
Accepted: 2025.02.17
Published: 2025.03.16

Assessment of photodegradation efficiency of selected antibiotics from WHO Watch group in environmental samples

Paulina Sowik[1*], Katarzyna Kowalska[1,2], Ewa Felis[1,2]

[1] Department of Environmental Biotechnology, Faculty of Energy and Environmental Engineering, Silesian University of Technology, ul. Akademicka 2, 44-100 Gliwice, Poland
[2] Biotechnology Centre, Silesian University of Technology, ul. B. Krzywoustego 8, 44-100 Gliwice, Poland
* Corresponding author's e-mail: paulina.sowik@polsl.pl

ABSTRACT

The widespread presence of antimicrobials in aquatic ecosystems, driven by human and agricultural activities, poses significant challenges to the environment and human health, particularly by facilitating the spread of antimicrobial resistance. This study investigated the solar-driven photodegradation of ciprofloxacin (CIP) and vancomycin (VAN) in real municipal wastewater effluent, using TiO_2-P25 and ZnO photocatalysts, with and without the addition of peroxymonosulfate (PMS). Experimental results demonstrate that CIP and VAN removal is significantly enhanced in the presence of PMS, achieving near-complete degradation within 5 minutes at a higher PMS concentration (200 mg L^{-1}) across all tested processes. These finding underscore the potential of PMS activation through photolysis and photocatalysis as an advanced strategy for mitigating antibiotics in complex environmental matrices, offering promising avenues for sustainable wastewater treatment. Further research is recommended to explore degradation pathways and assess the ecotoxicity of post-process solutions.

Keywords: ciprofloxacin, photocatalysis, peroxymonosulfate, vancomycin, wastewater treatment.

INTRODUCTION

The rapid expansion of urbanization and industrial activities has led to significant environmental challenges, notably the generation of wastewater containing a wide range of organic pollutants, including pharmaceuticals (Al Miad et al., 2024). Pharmaceutical contaminants, including antibacterials, enter water systems through improper disposal, agricultural irrigation, as well as consumption by humans, animals, and crops, posing serious threats to ecosystems (Fig. 1) (Samal et al., 2022). Due to their high polarity and low volatility, many pharmaceuticals are persistent in aquatic environments, making them more likely to accumulate in water bodies. Consequently, these compounds are often detected in wastewater treatment plant (WWTP) effluents, as conventional treatment methods are unable to fully remove them. Studies indicate that up to 90% of pharmaceutical residues may persist in treated wastewater (Deng et al., 2024; Ruziwa et al., 2023) and a significant amount of antibacterials that are not completely degraded accumulates in various environmental matrices, and their traces have been found in soil (0.66–760.1 µg kg^{-1}) (Deng et al., 2018), sediments (49.3 ± 24.7 ng g^{-1}) (Sharkey et al., 2024) and aquatic matrices (144–933 ng L^{-1}) (Qiu et al., 2024). Moreover, the presence of antibacterial residues in water bodies facilitates the emergence of antibiotic-resistance bacteria (ARB) and promotes the spread of antibiotics resistance genes (ARGs) among humans and other organisms [Srivastava, 2024]. AMR poses a critical global health challenge, causing over 1.27 million deaths annually. Addressing this issue requires minimizing the misuse and overuse of antibacterials to reduce the development and spread of AMR (Kim et al., 2024).

The World Health Organization (WHO) created AWaRe classification system to promote responsible antibiotic use, improve global stewardship, and combat AMR. By categorizing antibacterials into three groups – access, watch

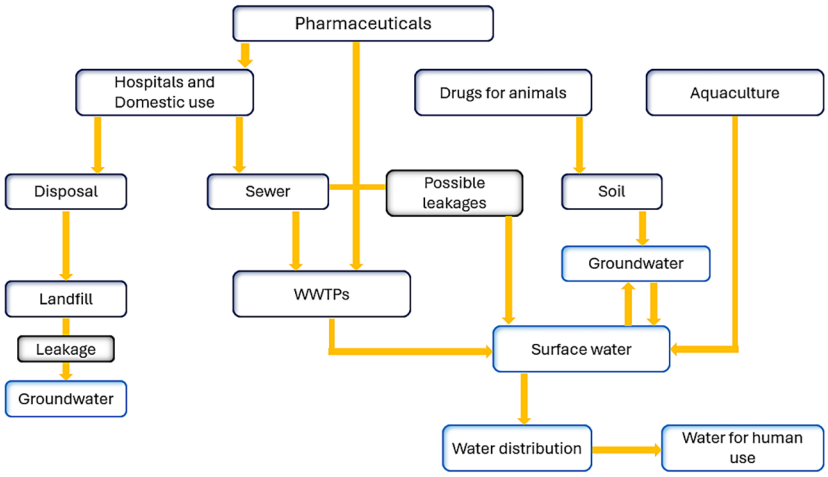

Figure 1. Pathways of pharmaceutical contaminants (based on Samal et al., 2022)

and reserve – the AWaRe framework aims to: i) guide prescribing practices; ii) monitor resistance trends and iii) safeguard critical drugs. The goal is to ensure effective treatments remain available while reducing the spread of resistant pathogens (WHO, 2022). There are many antibacterials that pose a threat to the environment, but among them, the ones that stand out in particular include: ciprofloxacin (CIP) and vancomycin (VAN). Both selected antibacterials are placed in the "watch group" by the WHO. This group includes antibacterials and antibacterial classes that have higher resistance potential and includes most of the highest priority agents among the Critically Important Antimicrobials for Human Medicine and/or antibacterials that are relatively high-risk selection of bacterial resistance (WHO, 2022). CIP is fluoroquinolone and constitutes one of the most frequently detected antibacterials in WWTP effluents, and its occurrence was also detected in environmental samples, such as river water (299.88 ng L^{-1}) (Praveena et al., 2018), groundwater (20.48 ng L^{-1}) (Arun et al., 2022), soil (0.32–84.85 µg kg^{-1}) (Sharifmand et al., 2024), and sludge (426 ng g^{-1}) (Li et al., 2013). VAN belongs to the glycopeptide class of antimicrobials and is an antibiotic used to treat Gram-positive bacterial infections and has also been used for human prophylaxis (Andriani et al., 2024; Wada et al., 2024). It has been classified as a "last-resort antibiotic", and this group includes the antibacterials that should be reserved for treatment of confirmed or suspected infections caused by multidrug-resistant bacteria. In France, VAN is strictly reserved for hospital use and could be a pertinent marker of hospital discharge as it was detected only in the hospital outflows (Louvet et al., 2017). However, after thirty years of glycopeptide use, vancomycin-resistant enterococci (VRE) emerged in 1986, because of the excessive exposure to VAN (Taučer-Kapteijn et al., 2016, Siegel, 2012). Recent findings identify urban and municipal WWTPs as significant contributors to the environmental spread of ARGs and ARB, including VRE (Biggel et al., 2021; Cherak et al., 2022; Oravcova et al., 2017; Valenza et al., 2024).

Taking this into account, it is essential to develop efficient wastewater treatment methods to remove antibacterials. Such approaches aim to reduce their environmental concentration, mitigate their ecological, as well as safeguard aquatic ecosystems by minimizing harm to fauna and flora (Szymańska et al., 2019). Conventional biological and mechanical wastewater treatment methods are unable to completely degrade certain micropollutants due to their inherent chemical stability and toxicity (Al Miad, et al. 2024). A potential solution to the challenges could involve the application of Advanced Oxidation Processes (AOPs), with particular emphasis on photocatalytic degradation using semiconductors (Wolski et al., 2021). At this moment, titanium dioxide (TiO_2) is the most often used semiconductor to produce charge carriers for photocatalytic processes of organic micropollutant degradation, due to its high effectiveness, non-toxic, and low costs. Zinc oxide (ZnO) is known as an alternative photocatalysts to TiO_2. One of the main disadvantages of this semiconductor is its photo-corrosion at low pH and low activity during exposition to sunlight (Bayan et al., 2021). Nevertheless, photodegradation of antimicrobials depends on

turbidity of water, because limited exposure to light in aquatic matrix, such as municipal wastewater effluent (MWWE), ZnO-based photocatalysis demonstrated higher efficiency than TiO_2-based photocatalysis towards antimicrobials like sulfonamides (Hussain et al., 2024, Kowalska et al., 2023). Consequently, ZnO is considered to have significant potential for applications in more complex matrices, such as environmental systems. However, despite achieving higher efficiency in the degradation of antimicrobials, complete degradation has not been attained in many cases, indicating that the use of well-known photocatalysts remains insufficient.

To overcome these limitations, advanced oxidation processes based on highly reactive sulfate radicals (SR-AOPs) were proposed, because of their strong oxidation ability and mineralization efficiency (Long et al., 2022). Sulfate radicals ($SO_4^{\bullet-}$) have multiple advantages over hydroxyl radicals (•OH) such as a higher selectivity, longer half-life and equal or higher redox potential (E0~ 3.1 V) (Li et al., 2021, Milh et al., 2021). In SR-AOPs, a diverse range of reactive species, including •OH, $SO_4^{\bullet-}$, superoxide anion ($O_2^{\bullet-}$) and singlet oxygen ($^1O_2$), can be generated to degrade organic compounds into CO_2, H_2O and other products (Jiang et al., 2022, Tian et al., 2023).

Peroxymonosulfate (PMS) serves as a key precursor for generating $SO_4^{\bullet-}$ in SR-AOPs. However, efficient radical generation from PMS for the degradation of most organic micropollutants poses significant challenges, due to high energy costs and poor activation performance. Therefore, there is a need to develop effective and environmentally friendly methods for PMS activation (He et al., 2022, Shen et al., 2020). Photocatalysis-assisted activation of PMS has emerged as a highly efficient approach for the removal persistent organic pollutants, such as antimicrobials (Li et al., 2024). For instance, Liu et al. (2021) demonstrated the synergistic effect of a (2D/2D) CoAl-LDH/BiOBr Z-scheme photocatalyst in combination with PMS/Vis system, achieving a 96% removal rate of CIP within 30 min. Moreover, $ZnFe_2O_4$ shows great potential to activate PMS and responds to visible light, because nearly complete degradation of CIP was achieved after 60 min [Zhang et al., 2022]. From an energy efficiency perspective, visible light-driven photocatalytic activation of PMS (Vis/catalyst/PMS) presents a highly promising strategy [Gu et al., 2024]. However, many newly proposed photocatalysts, despite their high efficiency in degrading antimicrobials, are costly to synthesize. Furthermore, studies are often conducted in simplified matrices, such as distilled water or Milli-Q water, which do not reflect the complexity of environmental aquatic medium.

Taking this into account, the main aim of this study was to assess the effectiveness of CIP and VAN removal in an environmental matrix – real municipal wastewater effluent (MWWE), via solar-driven photocatalytic processes, using TiO_2-P25 (as a reference semiconductor) and ZnO as an alternative photocatalysts. Experiments were conducted both without and in the presence of PMS at two different concentrations.

MATERIALS AND METHODS

Chemicals and reagents

Analytical standards of CIP (98%) and VAN-HC were obtained from Sigma Aldrich (China). Oxone salt ($KHSO_5$•$0.5KHSO_5$•$0.5K_2SO_4$) as PMS source was obtained from Sigma Aldrich (USA). Acetonitrile (ACN) for HPLC and formic acid (FA) ≥99.9% for LC-MS were supplied by VWR Chemicals (Poland). The studied photocatalysts: TiO_2-P25 (Titandioxid P25, 99.9%) and ZnO with purity 99.9% were supplied by Degussa (Germany) and Sigma-Aldrich (China), respectively. The solutions for mobile phase were prepared in 18.2 MΩ.cm Milli-Q water obtained from Synergy® Water Purification System (Merck, Germany).

Each of stock solutions of selected antimicrobials (10 mg L^{-1}) were prepared by dissolving 10 mg of its analytical standards in 1000 mL MWWE. CIP solution had to be stirred through 16 h in volumetric flask until analytical standard was completely dissolved. Working standard solutions in the concentration of 2 mg L^{-1} were prepared by dilution of 200 mL stock solutions in MWWE to appropriate concentration immediately before the use. Stock solutions were kept in the refrigerator (2°C) and were stable for at least 3 weeks.

Aquatic matrix

In the studies, real treated wastewater, i.e. municipal wastewater secondary effluent (MWWE), was selected as an environmental matrix for the tests. MWWE was collected from a municipal wastewater treatment plant (WWTP) located in Southern Poland, the area of Upper Silesia – one of the most urbanized

regions of the country. To remove suspended solids, the MWWE was pre-treated using filter paper. Characteristic physicochemical properties of the MWWE are presented in Table 1.

Analytical methods

Quantification of CIP and VAN

Selected antimicrobials were quantified using high-performance liquid chromatography (HPLC) equipped with a UV variable wavelength detector (UltiMate 3000 system; Dionex Corporation, Sunnyvale, CA, USA). All analyzed samples were filtered with MCMF-Millipore® membrane filters (0.22 µm pore size, Merck, Germany). C18 Hypersil™ Gold column (250 mm × 4.6 mm; 5 µm) utilized as the stationary phase, was purchased from Thermo Scientific (Polygen, Poland). The mobile phase consisted of 0.1% FA solution and ACN in a 77:23 (v/v) volumetric ratio. Analyses were performed at the maximum absorption wavelengths: 278 nm for CIP and 232 nm and 280 nm for VAN. The retention time (RT) of the target contaminants were 9.3 ± 0.5 min and 5.5 ± 0.8 min for CIP and VAN, respectively. The limit of quantification (LOQ) for the selected antimicrobials were 0.2 mg L^{-1} for CIP and 0.1 mg L^{-1} for VAN, set as the first calibration points on the calibration curve (linear regression, R2 > 0.98). Data were processed using Dionex Chromeleon™ 6.8 software.

Physicochemical properties of MWWE

Total organic carbon (TOC) and total nitrogen (TN) were determined in the filtered environmental sample with TOC-L Total Organic Carbon Analyzer and TNM-L Total Nitrogen Measuring Unit (Shimadzu, Japan), respectively. Ammonium nitrogen was measured using a Spectroquant NOVA 60™ spectrometer (Merck, Germany) and a spectrophotometric test purchased from Merck (kit no. 14752, Germany). The pH of the environmental sample was measured using a Multi 3510 IDS pH-meter (WTW, Germany). Other chemical properties were analyzed using Ion Chromatography Dionex Aquion (Thermo Scientific, Poland).

Table 1. Physicochemical properties of MWWE

Parameter	MWWE
TOC, mg L^{-1}	71.33
TN, mg L^{-1}	0.98
N-NH_4, mg L^{-1}	30.5 ± 2.12
N-NO_2, mg L^{-1}	0.41 ± 0.02
N-NO_3, mg L^{-1}	2.24 ± 0.18
P-PO_4, mg L^{-1}	0.55 ± 0.17
SO_4^{2-}, mg L^{-1}	116.11 ± 9.55
Cl^-, mg L^{-1}	177.65 ± 17.61
Br^-, mg L^{-1}	0.29 ± 0.02
F^-, mg L^{-1}	0.36 ± 0.06
pH	8.2

Experimental set-up

Sorption tests

To quantify the effect of adsorption of selected antibiotics onto photocatalysts surface, control experiments were performed under dark conditions. The experiments were carried out separately for each CIP and VAN, in beakers sealed tightly with aluminum foil to prevent any light exposure. Each test utilized a solution volume of 250 mL, with photocatalyst concentration of 20 mg L^{-1}, consistent with the conditions used in photocatalytic experiments. Antibiotics were continuously stirred using magnetic stirrers, and the tests were conducted over 60 minutes. Samples were collected at the same time intervals as in the photodegradation tests for consistent comparison.

Photodegradation experiments

Laboratory-scale experiments were conducted to investigate the removal of CIP and VAN in MWWE, under artificial sunlight conditions. A Solarbox 1500e solar simulator (Co.fo.me.gra, Italy), equipped with a 1500 W polychromatic xenon lamp was used to simulate solar radiation. The irradiation intensity was set at 500 W m^{-2}.

The study evaluated both photolytic and photocatalytic degradation of the selected antimicrobials under solar-driven conditions. Photocatalytic experiments were conducted using TiO_2-P25 and ZnO as photocatalysts, each at a concentration of 20 mg L^{-1}. PMS was applied at concentrations of 20 mg L^{-1} and 200 mg L^{-1} to investigate the effect of the sulfate anion precursor concentration on CIP and VAN degradation. In parallel, photolytic removal studies were performed to assess the susceptibility of CIP and VAN to decomposition under sunlight alone, without the addition of photocatalysts. These photolytic experiments were carried out under identical conditions to the photocatalytic processes. The effect of artificial solar irradiation on antimicrobial removal

was evaluated in selected matrix spiked with CIP and VAN (2 mg L^{-1}). For all experiments, the total solutions volume was 250 mL, and the irradiated area was 0.03 m^{-2}. Continuous stirring on magnetic stirrer was maintained throughout the process. Samples were collected at predetermined time intervals: 0, 5, 10, 20, 30, 45, 60, 90 min, and analyzed to monitor the degradation of antibiotics.

The removal efficiency of CIP and VAN (R_{CIP}, R_{VAN}) was calculated using following Eq. (1):

$$R_{CIP},R_{VAN} = \left(\frac{(C_0 - C_t)}{C_0}\right) \cdot 100\% \quad (1)$$

where: C_0 and C_t are the initial and residual antibiotics concentrations at time t (mg L^{-1}), respectively.

Kinetics calculations

The degradation kinetics of CIP and VAN followed a first-order model presented by Eqs. 2–3:

$$ln\left(\frac{C_t}{C_0}\right) = exp^{-k_t t} \quad (2)$$

$$t_{1/2} = \frac{ln2}{k_t} \quad (3)$$

where: C_t and C_0 are the concentration of selected antibiotics (mg L^{-1}) at time t and time 0, respectively; kt is the pseudo-first-order rate constant (min^{-1}) and t time (min). The time to achieve 50% antibiotics removal ($t_{1/2}$, min) was estimated in accordance with Eq. (3).

RESULTS AND DISCUSSION

Sorption tests

For ZnO, a slight decrease in the concentration of CIP was observed over 60 minutes [Figure 2]. This suggests that the interaction between CIP and ZnO is weak, potentially due to unfavorable surface chemistry. Meanwhile, Wolski et al. (2021) reported ca. 10% removal of CIP through sorption in deionized water within 60 minutes. Differences in the results may stem from the influence of a more complex matrix on the sorption process. In contrast, for CIP/TiO_2, a decrease in concentration was observed within the first 10 minutes, reaching approx. 16% removal. This indicates initial sorption of CIP onto TiO_2-P25. However, the concentration of CIP gradually increases, returning to values close to 100%. Du et al. (2019) similarly proved that TiO_2 demonstrated inferior adsorption efficiency towards CIP with 21.1%. This increase suggests desorption phenomena, where adsorbed CIP molecules are released back into the solution. The observed desorption may result from the dynamic equilibrium between sorption and desorption processes, likely driven by competition for active sites, or other environmental factors.

For VAN, sorption on both ZnO and TiO_2-P25 was insignificant, with the antibiotic concentration remaining close to 100% throughout the experiment. In the case of VAN sorption on TiO_2-P25, a slight decrease of approx. 5% was observed within the first 10 minutes, followed by a gradual return to initial concentration value. The weak

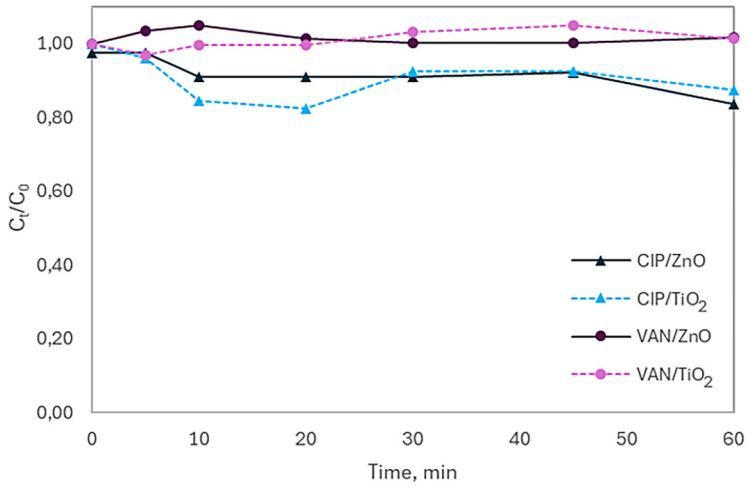

Figure 2. Removal of CIP and VAN from MWWE by sorption process using TiO_2-P25 and ZnO

interactions between VAN and photocatalysts might be attributed to steric factors associated with larger molecular structures of VAN or a lack of specific binding interactions with the surface.

Overall, the results indicate that both TiO_2-P25 and ZnO exhibit a higher sorption capacity for CIP compared to VAN. However, the desorption behavior for both antibiotics highlights the dynamic nature of the sorption-desorption equilibrium, which may be influenced by factors such as surface chemistry, molecular interactions, and environmental conditions. While ZnO demonstrates potential as a sorbent for removing antibiotics such as CIP from aqueous solutions, TiO_2-P25 shows promise for partial removal of CIP, albeit with limited retention due to desorption.

Photolysis

The photolysis of CIP and VAN was investigated under visible light, both in the presence and absence of PMS. The results indicate that photolysis alone archives moderate removal efficiency, with complete removal of CIP and only 22% removal of VAN after 30 minutes [Figure 3ab]. The kinetic parameters reveal a pseudo-first-order rate constant of 0.085 min^{-1} for CIP, whereas for VAN, k is significantly lower at 0.009 min^{-1} [Table 2].

The addition of PMS enhances photolytic degradation significantly. At a PMS concentration of 20 mg L^{-1}, CIP removal reaches 95% within 20 minutes, with an increased k value of 0.217 min^{-1}. VAN removal also improves, achieving 90% after 30 minutes, with pseudo-first-order constant increasing to 0.026 min^{-1}. Further increasing the PMS concentration to 200 mg L^{-1} results in near-complete degradation of both antibiotics. CIP exceeds complete removal within 5 minutes (k = 0.738 min^{-1}), while VAN achieves over 98% removal (k = 0.845 min^{-1}). These findings highlight the synergistic effect of PMS in enhancing photolytic degradation, particularly for the more resistant VAN molecule.

The results obtained in this study differ significantly from those reported in previous research. For instance, Zeng et al. (2021) reported ca. 3% removal rate of CIP after 150 minutes of photolysis in deionized water. Similarly, Du et al. (2019) observed negligible direct photodegradation of CIP in the absence of photocatalysts. Photolysis was also deemed ineffective for VAN removal, with <5% removal reported by Lofrano et al. (2018). These discrepancies can be attributed to various factors, including differences in the initial concentration of antibiotics and the complexity of the sample matrix.

In contrast, the current study demonstrated that photolysis can be highly efficient, even for compounds considered resistant to degradation, such as VAN. However, the effectiveness of photolysis is strongly influenced by the presence and concentration of PMS – the higher concentration of PMS, the greater the efficiency of antibiotic degradation. Specifically, complete degradation of both CIP and VAN were achieved within 5 minutes via photolysis in the presence of PMS at concentration of 200 mg L^{-1}. Supporting this finding, Jia et al. (2024) showed that increasing concentration of PMS enhanced the degradation rate of CIP, achieving removal rates of 39.2% and 93.1% after 80 minutes at PMS concentrations of 0.3 and 1 mM, respectively.

On the other hand, contradictory results have been observed in other studies. Another study reported only ca. 10.1% CIP degradation in deionized water within 60 minutes, even with a higher PMS concentration of 0.30 g L^{-1}. This limited efficiency has been attributes to the low redox potential of PMS under certain conditions (Yi et al., 2025). It is hypothesized that the presence of pre-existing sulfate ions in the sample matrix

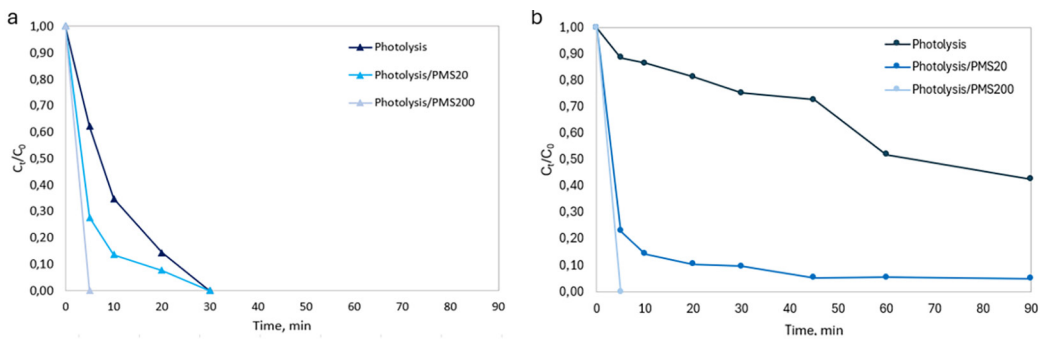

Figure 3. Solar-driven photolytic removal of (a) CIP; and (b) VAN from MWWE, both with and without PMS

may significantly influence the photodegradation process. This assumption is supported by results indicating that PMS exhibits greater efficiency in more complex matrices, where the interplay of matrix components may enhance photodegradation dynamics.

Photocatalysis in the presence of PMS

The photocatalytic degradation of CIP and VAN was examined using TiO_2-P25 and ZnO, with and without PMS (Fig. 4). For CIP, TiO_2 alone achieves a removal efficiency of 99% within 30 minutes, with a kinetic rate constant of 0.085 min^{-1} [Table 2]. The addition of PMS at 20 mg L^{-1} significantly enhances degradation, achieving over 80% removal within 10 minutes (k = 0.226 min^{-1}). At 200 mg L^{-1} PMS, complete degradation of CIP was achieved within 5 minutes (k = 0.921 min^{-1}). For VAN, TiO^2 alone results in only 55% after 90 minutes (k = 0.017 min^{-1}). With PMS at 20 mg L^{-1}, removal efficiency increases to over 83% (k = 0.032 min^{-1}). At 200 mg L^{-1} PMS, complete removal was achieved after 5 minutes (k = 0.764 min^{-1}), demonstrating the strong oxidizing power of PMS in conjunction with TiO_2-based photocatalysis.

For CIP, ZnO-based photocatalysis achieves a removal efficiency of 99% within 30 minutes (k = 0.086 min^{-1}). The addition of PMS at 20 mg L^{-1} further increases the removal efficiency to approx. 80% within 5 minutes (k = 0.226 min^{-1}). At 200 mg L^{-1} of PMS concentration, near-complete degradation occurs within 5 minutes (k = 0.921 min^{-1}). For VAN, ZnO alone achieves a modest removal of 66% after 60 minutes (k = 0.017 min^{-1}). The presence of 20 mg L^{-1} PMS enhances removal to 99% (k = 0.032 min^{-1}), while at 200 mg L^{-1} of PMS, removal improves to complete degradation after 5 minutes (k = 0.764 min^{-1}).

The results demonstrate that PMS significantly enhances the degradation of both CIP and VAN during photolysis and photocatalysis, with ZnO and TiO_2 performing comparably. However, CIP degradation is consistently more efficient than VAN due to the differences in molecular structure and reactivity. TiO_2 and ZnO exhibit strong potential as photocatalysts, particularly when combined with sulfate anion radical precursor, such as PMS.

In principle, photocatalysis addresses the limited efficiency of photolysis by significantly enhancing the degradation rate. For instance, addition of TiO_2 has been shown to increase the efficiency of CIP degradation from ca. 0 to 42–47.1% (Zeng et al., 2020, Du et al., 2019). TiO_2-based photocatalysis has also demonstrated high photodegradation activity under visible light, achieving approx. 70% removal of CIP (Yang et al., 2016). Similarly, a ZnO-based photocatalysis system achieved 70-85% VAN degradation in deionized

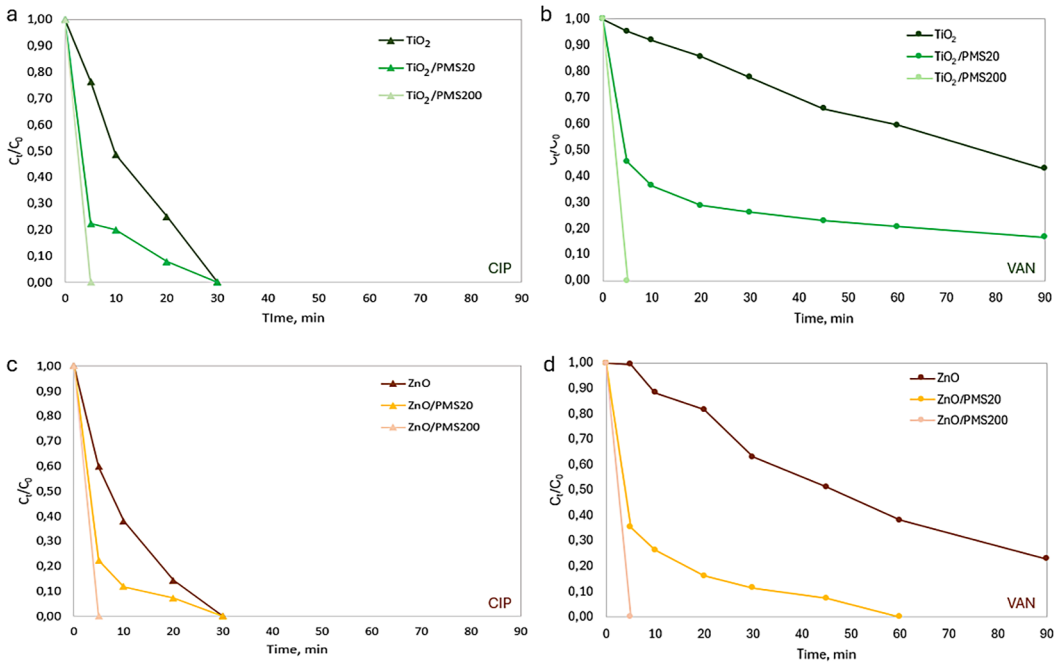

Figure 4. Solar-driven photocatalytic degradation of (a) CIP using TiO_2-P25 and (c) ZnO; (b) VAN using TiO_2-P25 and d) ZnO

water within 10 minutes and TiO_2-based photocatalysis system yielded 59-73% degradation within 90 minutes (Lofrano et al., 2018). Rahrovan et al. (2024) further reported remarkably high VAN degradation efficiencies using ZnO photocatalysts, although the efficiency declined significantly in real raw sewage matrices (13 and 24%).

In contrast, the current study indicates that the addition of photocatalysts alone does not enhance the degradation rates of CIP and VAN. Instead, the presence of PMS improves removal efficiency. However, other studies suggest limitations in certain systems. For example, Yi et al. (2025) reported that a ZnO/PMS system achieved less than 30% CIP removal, while Longfei et al. (2024) observed only 7.2% CIP degradation using a TiO_2/PMS system in deionized water. Notably, only the Vo-CTNs system with 1 mM PMS achieved a 97.5% removal rate. Furthermore, the same study demonstrated that increasing PMS concentrations beyond 1 mM did not result in further efficiency improvements.

It is important to note that the research discussed was conducted in pure aquatic matrices, such as deionized water. The studies examining the effects of environmental matrices on photodegradation efficiency driven by visible light, especially with PMS, remain scarce. This study highlighted the potential of a properly optimized PMS concentration to efficiently degrade even complex molecules such as VAN in MWWE within 5 minutes. These findings underscore the high potential of PMS as a sulfate radical precursor for combating organic micropollutants, including antimicrobials.

CONCLUSIONS

This study highlighted the efficiency of ZnO and TiO_2-P25 photocatalysts in the degradation of CIP and VAN under various conditions, including sorption, photolysis, and photocatalysis, with and without the presence of PMS.

ZnO and TiO_2-P25 showed higher sorption affinity for CIP compared to VAN, as evidenced by the initial decrease in CIP concentration. However, desorption phenomena were observed, indicating a dynamic sorption-desorption process influenced by molecular interactions. VAN exhibits negligible sorption on both ZnO and TiO_2-P25, possibly due to steric hindrance and lack of strong binding interactions.

The photolysis process demonstrated moderate removal efficiency, with complete degradation of CIP and 22% removal of VAN after 30 minutes. The addition of PMS significantly enhanced photolysis, particularly for the more resistant VAN molecule. At a PMS concentration of 200 mg L^{-1}, near complete degradation of both antibiotics was achieved within 5 minutes, demonstrating the synergistic effect of PMS in generating reactive oxidizing species.

TiO_2-P25 and ZnO exhibited strong photocatalytic activity, with the removal efficiencies for CIP and VAN being significantly enhanced by the presence of PMS. Without PMS, TiO_2-P25 achieved 99% removal of CIP within 30 minutes and 55% removal of VAN within 90 minutes. ZnO-based photocatalysis showed comparable results. The addition of PMS (20 mg L^{-1}) significantly increased removal rates for both antibiotics, achieving over 80% removal within 10 minutes for CIP and over 83% removal for VAN. At 200 mg L^{-1} PMS, both antibiotics were completely degraded within 5 minutes, with TiO_2-P25 and ZnO.

CIP degradation was consistently more efficient than VAN under all conditions, highlighting the influence of molecular structure on reactivity. The larger, more complex structure of VAN reduces its interaction with photocatalysts, and ROS generated during photolysis and photocatalysis.

These results underscore the strong potential of photodegradation of antibiotics in complex aqueous environments, like MWWE. The addition of PMS as a sulfate radical precursor significantly enhances the degradation efficiency, making it a promising strategy for mitigating the environmental impact of pharmaceutical micropollutants. The synergistic use of PMS with ZnO or TiO_2-based photocatalysis represents a highly effective strategy for the removal of antibiotics from environmental aquatic matrices, with implication for sustainable water purification practices. However, the study results indicated that the use of PMS alone, but at higher concentrations, enabled effective removal of both CIP and VAN from a complex aqueous matric, specifically treated real municipal wastewater. This suggests the potential application of PMS as a standalone treatment in environmental matrices for the removal of micropollutants, such as antibiotics.

Future research should focus on identifying and analyzing the degradation pathways and transformation products formed during photodegradation processes, as these intermediates

may exhibit higher toxicity than the parent compounds. Additionally, comprehensive ecotoxicity assessments of post-process solutions are crucial to ensure that the treatment method is safe, and produced byproducts do not exhibit higher toxicity than the parent compounds.

Acknowledgements

This work was supported by Silesian University of Technology under 2024 grant with no. 08/070/BKM24/0032 (BKM-714/RIE7/2024) and 2025 grant with no. 08/070/BK_25/0038.

REFERENCES

1. Al Miad A., Saikat S. P., Alam M. K., Sahadat Hossain M., Bahadur N. M., & Ahmed S. (2024). Metal oxide-based photocatalysts for the efficient degradation of organic pollutants for a sustainable environment: a review. *Nanoscale Advances*, 4781–4803. https://doi.org/10.1039/d4na00517a
2. Andriani L., Rega M., Bonilauri P., Pupillo G., De Lorenzi G., Bonardi S., Conter M., & Bacci C. (2024). Vancomycin resistance and virulence genes evaluation in Enterococci isolated from pork and wild boar meat. *Heliyon*, *10*(14), e34543. https://doi.org/10.1016/j.heliyon.2024.e34543
3. Arun S., Xin L., Gaonkar O., Neppolian B., Zhang G., & Chakraborty P. (2022). Antibiotics in sewage treatment plants, receiving water bodies and groundwater of Chennai city and the suburb, South India: Occurrence, removal efficiencies, and risk assessment. *Science of the Total Environment*, *851*, 158195. https://doi.org/10.1016/j.scitotenv.2022.158195
4. Bayan E. M., Pustovaya L. E., & Volkova M. G. (2021). Recent advances in TiO_2-based materials for photocatalytic degradation of antibiotics in aqueous systems. *Environmental Technology and Innovation*, *24*, 101822. https://doi.org/10.1016/j.eti.2021.101822
5. Biggel M., Nüesch-Inderbinen M., Raschle S., Stevens M. J. A., & Stephan R. (2021). Spread of vancomycin-resistant Enterococcus faecium ST133 in the aquatic environment in Switzerland. *Journal of Global Antimicrobial Resistance*, *27*, 31–36. https://doi.org/10.1016/j.jgar.2021.08.002
6. Cherak Z., Bendjama E., Moussi A., Benbouza A., Grainat N., Rolain J. M., & Loucif L. (2022). First detection of vanA positive Enterococcus faecium clonal complex 17 in hospital wastewater in Algeria: an epidemiological report. *New Microbes and New Infections*, *47*, 100977. https://doi.org/10.1016/j.nmni.2022.100977
7. Deng J., Zhang W., Zhang L., Qin C., Wang H., & Ling,W. (2024). Micro-interfacial behavior of antibiotic-resistant bacteria and antibiotic resistance genes in the soil environment: A review. *Environment International*, *191*, 108972. https://doi.org/10.1016/j.envint.2024.108972
8. Deng Y., Li B., & Zhang T. (2018). Bacteria That make a meal of sulfonamide antibiotics: blind spots and emerging opportunities. *Environmental Science and Technology*, *52*(7), 3854–3868. https://doi.org/10.1021/acs.est.7b06026
9. Du J., Ma S., Yan Y., Li K., Zhao F., & Zhou J. (2019). Corn-silk-templated synthesis of TiO_2 nanotube arrays with Ag_3PO_4 nanoparticles for efficient oxidation of organic pollutants and pathogenic bacteria under solar light. *Colloids and Surfaces A: Physicochemical and Engineering Aspects*, *572*, 237–249. https://doi.org/10.1016/j.colsurfa.2019.04.018
10. Gu D., Liu Y., Zhu H., & Hao J. (2024). Cobalt-doped iron-based metal–organic gels as efficient visible-light-driven peroxymonosulfate activators for the efficient degradation of norfloxacin with simultaneous antibacterial activity. *Chemical Engineering Journal*, *486*, 149892. https://doi.org/10.1016/j.cej.2024.149892
11. He Y., Qioan J., Wang P., Wu J., Lu B., Tang S., Gao P., (2022). Acceleration of levofloxacin degradation by combination of multiple free radicals via MoS_2 anchored in manganese ferrite doped perovskite activated PMS under visible light. Chemical Engineering Journal, *431*, 133933. https://doi.org/10.1016/j.cej.2021.133933
12. Hussain S., Butt T. E., Akram H., & Fida H. (2024). Life cycle of medicinal compounds from life saving to life threating component in environment – Innovative use of nanotechnology for treatment. *Cleaner Water*, *2*, 100046. https://doi.org/10.1016/j.clwat.2024.100046
13. Jia X., Zhang J., Huang Q., Xiong C., Ji H., Ren Q., Jin Z., Chen S., Guo W., Chen J., Ge Y., & Ding Y. (2024). Efficient degradation of ciprofloxacin in wastewater by $CuFe_2O_4$/CuS photocatalyst activated peroxynomosulfate. *Environmental Research*, *241*(October 2023), 117639. https://doi.org/10.1016/j.envres.2023.117639
14. Jiang, Z. R., Li, Y., Zhou, Y. X., Liu, X., Wang, C., Lan, Y., & Li, Y., (2022). Co3O4-MnO2 nanoparticles moored on biochar as a catalyst for activation of peroxymonosulfate to efficiently degrade sulfonamide antibiotics. S*eparation and Purification Technology*, *281*, 119935. https://doi.org/10.1016/j.seppur.2021.119935
15. Kim J. I., Manuele A., Maguire F., Zaheer R., McAllister T. A., & Beiko R. (2024). Identification of key drivers of antimicrobial resistance in

Enterococcus using machine learning. *Canadian Journal of Microbiology*, *460*(2021), 446–460. https://doi.org/10.1139/cjm-2024-0049

16. Kowalska K., Sowik P., Bartolewski W., Ahmed H., Felis E., (2024). Solar-driven photocatalytic removal of anti-microbial drugs – Comparison of the efficiency of selected photocatalysts. *Desalination and Water Treatment*, *317*, 100275. https://doi.org/10.1016/j.dwt.2024.100275
17. Li J., Shang E., Li X., Tian J., Xu Z., & Li J. (2024). Efficient ofloxacin degradation via peroxymonosulfate activation using an S-scheme MoS_2/Co_3O_4 heterojunction composite under visible light: Performance and mechanistic insights. *Environmental Research*, *262*(P2), 119891. https://doi.org/10.1016/j.envres.2024.119891
18. Li D., Zhang N., Yuan R., Chen H., Wang F., & Zhou B., (2021). Effect of wavelengths on photocatalytic oxidation mechanism of sulfadiazine and sulfamethoxazole in the presence of TiO_2. *Journal of Environmental Chemical Engineering*, *9*, 106243. https://doi.org/10.1016/j.jece.2021.106243
19. Li W., Shi Y., Gao L., Liu J., & Cai Y. (2013). Science of the Total Environment Occurrence, distribution and potential affecting factors of antibiotics in sewage sludge of wastewater treatment plants in China. *Science of the Total Environment*, *445–446*, 306–313. https://doi.org/10.1016/j.scitotenv.2012.12.050
20. Liu C., Mao S., Shi M., Wang F., Xia M., Chen Q., & Ju X. (2021). Peroxymonosulfate activation through 2D/2D Z-scheme CoAl-LDH/BiOBr photocatalyst under visible light for ciprofloxacin degradation. *Journal of Hazardous Materials*, *420*, 126613. https://doi.org/10.1016/j.jhazmat.2021.126613
21. Lofrano G., Ozkal C. B., Carotenuto M., & Meric S. (2018). Comparison of TiO_2 and ZnO catalysts for heterogenous photocatalytic removal of vancomycin B. *Advances in Environmental Research-an International Journal*, *7*(3), 213–223. https://doi.org/10.12989/aer.2019.7.3.213
22. Long L., Bai C., Zhou X., Zhang S., Zhang Y., Chen C., He J., Song C., & Yang G., (2022). A novel strategy for promoting PMS activation: Enhanced utilization of side reactions. *Separation and Purification Technology*, *297*, 121432. https://doi.org/10.1016/j.seppur.2022.121432
23. Longfei W., Weijie W., Li L., Zhenhua W., Xing H., Linlin W., Fangjie Z., Yi L., & Haijiao X. (2024). Activation of peroxymonosulfate for ciprofloxacin degradation by a novel oxygen-deficient $CoTiO_3$/TiO_2NTs/Ti composite catalytic membrane: Electron transfer pathway and underlying mechanism. *Separation and Purification Technology*, *330*. https://doi.org/10.1016/j.seppur.2023.125511
24. Louvet J. N., Carrion C., Stalder T., Alrhmoun M., Casellas M., Potier O., Pons M. N., & Dagot C. (2017). Vancomycin sorption on activated sludge Gram+ bacteria rather than on EPS; 3D Confocal Laser Scanning Microscopy time-lapse imaging. *Water Research*, *124*, 290–297. https://doi.org/10.1016/j.watres.2017.07.056
25. Milh H., Cabooter D., & Dewil R., (2021). Role of process parameters in the degradation of sulfamethoxazole by heat-activated peroxymonosulfate oxidation: Radical identification and elucidation of the degradation mechanism. *Chemical Engineering Journal*, *422*, 130457. https://doi.org/10.1016/j.cej.2021.130457
26. Oravcova V., Mihalcin M., Zakova J., Pospisilova L., Masarikova M., & Literak I. (2017). Vancomycin-resistant enterococci with vanA gene in treated municipal wastewater and their association with human hospital strains. *Science of the Total Environment*, *609*, 633–643. https://doi.org/10.1016/j.scitotenv.2017.07.121
27. Praveena S. M., Shaifuddin S. N. M., Sukiman S., Nasir F. A. M., Hanafi Z., Kamarudin N., Ismail T. H. T., & Aris A. Z. (2018). Pharmaceuticals residues in selected tropical surface water bodies from Selangor (Malaysia): Occurrence and potential risk assessments. *Science of the Total Environment*, *642*, 230–240. https://doi.org/10.1016/j.scitotenv.2018.06.058
28. Qiu X., Pu M., Zhang H., Xu B., Wang J., & Xuan R. (2024). Occurrence, distribution, and correlation of antibiotics in the aquatic ecosystem of Poyang Lake Basin, China. *Journal of Hazardous Materials*, *479*, 135656. https://doi.org/10.1016/j.jhazmat.2024.135656
29. Rahrovan M., Rahmani H., Rabbani D., Miranzadeh M., & Rahimi H. (2024). Optimization of vancomycin antibiotic removal from synthetic and real wastewater using UV/Fe_3O_4@Alg-ZnO nanocomposite photocatalysis: response surface methodology based on a box-behnken design. *Health and Development Journal*, *13*(1), 1–10. https://doi.org/10.34172/jhad.92360
30. Ruziwa D. T., Oluwalana A. E., Mupa M., Meili L., Selvasembian R., Nindi M. M., Sillanpaa M., Gwenzi W., & Chaukura N. (2023). Pharmaceuticals in wastewater and their photocatalytic degradation using nano-enabled photocatalysts. *Journal of Water Process Engineering*, *54*, 103880. https://doi.org/10.1016/j.jwpe.2023.103880
31. Samal K., Mahapatra S., & Hibzur Ali M. (2022). Pharmaceutical wastewater as Emerging Contaminants (EC): Treatment technologies, impact on environment and human health. *Energy Nexus*, *6*, 100076. https://doi.org/10.1016/j.nexus.2022.100076
32. Sharifmand M., Sepehr E., Rasouli-Sadaghiani M. H., Asri-Rezaei S., & Rengel Z. (2024). Antibiotics

pollutants in agricultural soil: Kinetic, sorption, and thermodynamic of ciprofloxacin. *Heliyon*, *10*(18), e37035. https://doi.org/10.1016/j.heliyon.2024.e37035

33. Sharkey M., Stubbings W. A., Harrad S., Healy M. G., Wang S., Jin J., & Coggins A. M. (2024). Antibiotics residues in inland and transitional sediments. *Chemosphere*, *369*, 143793. https://doi.org/10.1016/j.chemosphere.2024.143793
34. Shen AH., Wen XJ., Fei ZH., Liu ZT., Mu QM., (2020). Visible-light-driven activation of peroxymonosulfate for accelerating ciprofloxacin degradation using CeO_2/Co_3O_4 p-n heterojunction photocatalysts. *Cheimcal Engineering Journal*. 2020;391:123612.
35. Siegel J.D., (2012). 2 - Pediatric Infection Prevention and Control, Editor(s): Sarah S. Long, Principles and practice of pediatric infectious diseases (Fourth Edition), 9–24.e3
36. Srivastava S. K. (2024). Recent advances in removal of pharmaceutical pollutants in wastewater using metal oxides and carbonaceous materials as photocatalysts: a review. *RSC Applied Interfaces*, *1*(3), 340–429. https://doi.org/10.1039/d3lf00142c
37. Szymańska U., Wiergowski M., Sołtyszewski I., Kuzemko J., Wiergowska G., & Woźniak M. K. (2019). Presence of antibiotics in the aquatic environment in Europe and their analytical monitoring: Recent trends and perspectives. *Microchemical Journal*, *147*, 729–740. https://doi.org/10.1016/j.microc.2019.04.003
38. Taučer-Kapteijn M., Hoogenboezem W., Heiliegers L., de Bolster D., & Medema G. (2016). Screening municipal wastewater effluent and surface water used for drinking water production for the presence of ampicillin and vancomycin resistant enterococci. *International Journal of Hygiene and Environmental Health*, *219*(4–5), 437–442. https://doi.org/10.1016/j.ijheh.2016.04.007
39. The WHO AWaRe (Access, Watch, Reserve) antibiotics book, ISBN 978-92-4-006238-2 (online access: 16.12.24)
40. Tian N., Giannakis S., Akbarzadeh L., Hasanvandian F., Dehghanifard E., & Kakavandi B., (2023). Improved catalytic performance of ZnO via coupling with $CoFe_2O_4$ and carbon nanotubes: A new, photocatalysis-mediated peroxymonosulfate activation system, applied towards Cefixime degradation. *Journal of Environmental Management*, *329*, 117022. https://doi.org/10.1016/j.jenvman.2022.117022
41. Valenza G., Eisenberger D., Esse J., Held J., Lehner-Reindl V., Plaumann P.-L., Ziegler T., Knauer M., Bogdan C., & Dudler P. (2024). High prevalence of the recently identified clonal lineage ST1299/CT3109 vanA among vancomycin-resistant Enterococcus faecium strains isolated from municipal wastewater. *MSphere*, *9*(9). https://doi.org/10.1128/msphere.00396-24
42. Wada Y., Ibrahim A. B. Umar Y. A., Afolabi H. A., Wada M., Alissa M., Al Amri K. A. S., AL Ibrahim A. A., Al Fares M. A., Albayat H., AlKhathlan M. K., Al Kaabi N. A., Al-Subaie M. F., Alfaresi M., Alrasheed H. A., Rabaan A. A., Yean C. Y., & Zaidah A. R. (2024). Status of vancomycin-resistant Enterococcus in species of wild birds: A systematic review and meta-analysis. *Journal of Infection and Public Health*, *17*(6), 1023–1036. https://doi.org/10.1016/j.jiph.2024.04.004
43. Wolski L., Grzelak K., Muńko M., Frankowski M., Grzyb T., & Nowaczyk G. (2021). Insight into photocatalytic degradation of ciprofloxacin over CeO_2/ZnO nanocomposites: Unravelling the synergy between the metal oxides and analysis of reaction pathways. *Applied Surface Science*, *563*. https://doi.org/10.1016/j.apsusc.2021.150338
44. Yang Z., Yan J., Lian J., Xu H., She X., Li H., (2016). g-C_3N_4/TiO_2 nanocomposites for degradation of ciprofloxacin under visible light irradiation. *Chemistry Select*. *1*(18), 5679–5685. https://doi.org/10.1002/slct.201600861
45. Yi M., Shang J., Zhang S., Gan X., Song Shang C., Xu S., Liu Y., Feng D., & Cheng X. (2025). Peroxymonosulfate activation by ZnO-$ZnMnO_3$/CuS nanocomposite for efficient degradation of ciprofloxacin based on a non-radical pathway: The promoting effect of CuS on electron transfer. *Chemical Engineering Journal*, *504*, 158885. https://doi.org/10.1016/j.cej.2024.158885
46. Zhang S, Guo R, Liang M, Li L, (2022). Regulation of $ZnFe_2O_4$ synthesis for optimizing photoelectric response and its application for ciprofloxacin degradation: The synergistic effect with peroxymonosulfate and visible light, P*rocess Safety and Environmental Protection*, *165*, 323–335. https://doi.org/10.1016/j.psep.2022.07.003
47. Zeng X. feng, Wang J. sheng, Zhao Y. na, Zhang W. li, & Wang M. huan. (2021). Construction of TiO_2-pillared multilayer graphene nanocomposites as efficient photocatalysts for ciprofloxacin degradation. *International Journal of Minerals, Metallurgy and Materials*, *28*(3), 503–510. https://doi.org/10.1007/s12613-020-2193-y